Simulation and verification of improved particle swarm optimization for maximum power point tracking in photovoltaic systems under dynamic environmental conditions

**Muhammad Khairul Azman Mohd Jamhari, Norazlan Hashim, Rahimi Baharom,
Muhammad Murtadha Othman**

School of Electrical Engineering, College of Engineering, Universiti Teknologi MARA, Shah Alam, Malaysia

Article Info	ABSTRACT
	This paper introduces an improved particle swarm optimization (iPSO) algorithm designed for maximum power point tracking (MPPT) in photovoltaic (PV) systems. The proposed algorithm incorporates a novel reinitialization mechanism that dynamically detects and adapts to environmental changes. Additionally, an exponentially decreasing inertia weight is utilized to balance exploration and exploitation, ensuring rapid convergence to the global maximum power point (GMPP). A deterministic initialization strategy is employed to uniformly distribute particles across the search space, thereby increasing the likelihood of identifying the GMPP. The iPSO algorithm is thoroughly evaluated using a MATLAB/Simulink simulation and validated with real-time hardware, including a boost DC-DC converter, dSPACE, and a Chroma PV simulator. Comparative analysis with conventional PSO and PSO-reinit algorithms under various irradiance patterns demonstrates that the iPSO consistently outperforms in terms of convergence speed and MPPT efficiency. The study highlights the robustness of the iPSO algorithm in bridging theoretical models with practical applications.

Corresponding Author:

Norazlan Hashim
School of Electrical Engineering, College of Engineering, Universiti Teknologi MARA
40450 Shah Alam, Malaysia
Email: azlan4477@uitm.edu.my

1. INTRODUCTION

Solar energy has emerged as a critical solution to global energy challenges, offering a renewable and environmentally friendly alternative to traditional energy sources [1]. The photovoltaic (PV) effect, which directly converts solar radiation into electricity with the help of semiconductor positive-type and negative-type (pn) junctions, forms the basis of solar power generation. However, the efficiency of PV systems is highly susceptible to environmental factors such as irradiance and temperature, resulting in nonlinear power–voltage (P–V) and current–voltage (I–V) characteristic curves in PV cells.

To maximize the efficiency of PV systems, maximum power point tracking (MPPT) algorithms are employed [2], [3]. These algorithms are integrated into DC–DC converters to extract the maximum available power under varying environmental conditions. Traditional algorithms such as perturb and observe (P&O), hill climbing (HC), and incremental conductance (INC) [4]-[11] are popular due to their simplicity and effectiveness under uniform irradiance, but they struggle with partial shading conditions (PSC) where multiple local maximum power points (LMPPs) exist [12]-[14].

In response to the limitations of conventional algorithms, artificial intelligence (AI)-based MPPT algorithms have been developed. Among these, the particle swarm optimization (PSO) technique has gained significant attention due to its simplicity and robustness [15]. However, conventional PSO algorithms suffer from stagnation [16] when not properly adapted to changing environments, and often converge to local rather than global maximum power points, especially with a small number of particles [17].

To overcome these challenges, this paper presents an improved PSO (iPSO) MPPT algorithm. The iPSO algorithm includes a real-time mechanism to detect dynamic environmental changes and reinitialize MPPT when significant irradiance changes occur. It exponentially decreases the inertia weight to balance exploration and exploitation, thereby accelerating convergence. Additionally, it employs a deterministic initialization strategy to distribute particles uniformly across the search space, increasing the likelihood of finding the global maximum power point.

To assess the effectiveness of the proposed iPSO algorithm, a stand-alone PV system with a boost DC-DC converter is developed in MATLAB/Simulink and validated in real-time hardware using a DS1104 dSPACE (control desk) and a Chroma 62000 H PV simulator. The iPSO's performance is compared to existing algorithms under uniform irradiance, rapid irradiance step changes, and partial shading conditions. This paper is organized as follows: section 2 outlines the methodology, including the implementation of the iPSO; section 3 provides an overview of the system; sections 4 and 5 cover the simulation and hardware setup, respectively; section 6 presents the results and discussion; and section 7 concludes the study.

2. METHODOLOGY
2.1. Implementation of iPSO method
Particle swarm optimization (PSO) is an artificial intelligence optimization technique inspired by the collective behavior of birds and fish. In PSO, potential solutions are represented as particles within a multidimensional search space, where they adjust their positions based on both their individual best-known positions and the best-known positions within the swarm. The conventional PSO algorithm incorporates an inertia weight, as introduced by Shi and Eberhart in 1998, to balance the trade-off between exploration and exploitation [18]. The iPSO algorithm developed in this research builds upon the conventional PSO by integrating a novel mechanism aimed at enhancing optimization efficiency. This mechanism, illustrated in Figure 1, addresses the inherent limitations of the conventional PSO. The following section will provide a detailed discussion of this novel mechanism and its impact on the optimization process.
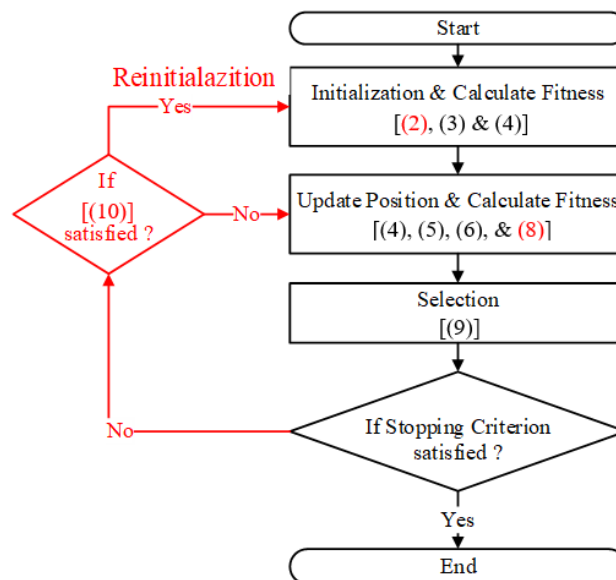

Figure 1. Flowchart of the iPSO optimization process

2.2. Initialization and fitness calculation
The initialization and fitness calculation process begins by randomly generating a predefined number of particles (NP) within the boundaries of the search space, as outlined in (1).

$$for \quad i = 1: NP$$
$$x_i^{k-1} = LB + (UB - LB) \times rand \cdot i \tag{1}$$
$$end$$

Here, (x) represents the initial position of the $(k\text{-}1)$ particle, LB and UB signify the lower and upper bounds of the search space respectively, and rand is a randomly generated number from a uniform distribution between 0 and 1.

The (1) specifies that each particle's position corresponds to the duty cycle of the converter, constrained between 0 and 1. Due to the inherent stochastic nature of the PSO algorithm, particles may initiate their search from suboptimal positions, which could potentially slow down convergence to the global optimum. To mitigate this issue, increasing the number of particles (NP) is often recommended; however, this approach can result in reduced tracking speed. This trade-off is addressed by implementing a deterministic initialization method (DIM), as described in [19] and illustrated in (2):

$$for \quad i = 0: (NP - 1)$$
$$x_i^{k-1} = [LB + 0.1 \cdot (UB - LB)] + \left[0.8 \cdot \frac{(UB-LB)}{(NP-1)}\right] \cdot i \tag{2}$$
$$end$$

Furthermore, the initial velocity of each particle (x_i^{k-1}) is randomly assigned within 20% of the designated velocity range, adhering to the constraint in (3):

$$v_i^{k-1} = v(vmin_{max} \times rand \times 0.2)_{min} \tag{3}$$

Here, v_{min} and v_{max} are the predetermined lower and upper velocity limits, respectively. Subsequently, the fitness of each particle is assessed using the objective function $f(x)$, as specified in (4):

$$f(x) = max\big(P_{PV}(x) = V_{PV}(x) \times I_{PV}(x)\big) \tag{4}$$

where V_{PV}, I_{PV}, and P_{PV} are the PV array output voltage, current and power, respectively.

2.3. Update position and fitness calculation

Each particle within the algorithm iteratively explores the search space to identify the optimal solution by updating its position (x) and velocity (v) as outlined in (5):

$$x_i^k = x_i^{k-1} + v_i^k \tag{5}$$

where x_i^k and v_i^k are the position and velocity of the ith particle at iteration (k), respectively. v_i^k, as described in (5), is influenced by both the individual's best historical position (P_{best}) and the best-known position among all particles in the swarm (G_{best}). This dual influence aims to balance individual learning and social learning within the swarm. The updated velocity is calculated as follows:

$$v_i^k = w^{k-1} \cdot v_i^{k-1} + c_1 \cdot rand\big(P_{best}^{k-1} - x_i^{k-1}\big) + c_2 \cdot rand\big(G_{best}^{k-1} - x_i^{k-1}\big) \tag{6}$$

where ω^{k-1} is the inertia weight controlling the velocity at iteration $(k\text{-}1)$; c_1 and c_2 are the acceleration constants that govern relative velocity with respect to P_{best} and G_{best}, respectively.

To effectively manage the exploration-exploitation trade-off during the optimization process, the inertia weight ω is dynamically adjusted. A larger ω promotes broader search behavior, facilitating global exploration, while a smaller ω enhances the particle's ability to fine-tune its search around its best-known position, thereby supporting local exploitation. Typically, the adjustment of ω is implemented by linearly decreasing its value over the course of iterations, as illustrated in (7):

$$w^{k+1} = \left(wmin_{max}\left(\frac{Iter_{max}}{Iter_{max}} + w_{min}\right)\right) \tag{7}$$

where ω_{max} and ω_{min} are the maximum and minimum values of ω, respectively; $Iter_{max}$ is the maximum number of iterations; and (k) and $(k+1)$ are the current and next iteration numbers, respectively.

In this research, to accelerate convergence to the optimal solution, the inertia weight ω is dynamically reduced according to an exponential decay model, as detailed in (8). This model is depicted in Figure 2, which compares the convergence profiles of inertia weight decay using both linear and exponential methods ((7) and (8), respectively). Following each iteration, the fitness of a particle is assessed using the function described previously in (4):

$$w^{k+1} = (wmin_{max}(1 - \delta)^k + w_{min}) \tag{8}$$

where δ is the decay rate, which in this study is set at 0.45.
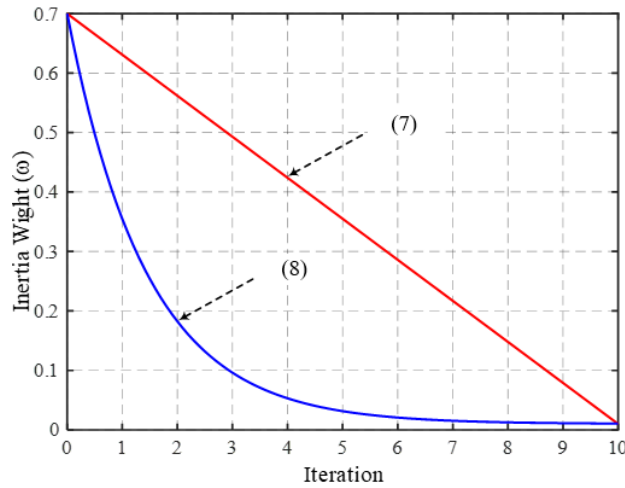
Figure 2. Convergence plot of ω

2.4. Selection

In the selection phase of this study, the tournament selection method is employed to determine which particles advance to the subsequent iteration. This method was chosen for its simplicity and ease of implementation. It involves a comparative evaluation in which particles from the current iteration are matched against those from the previous iteration based on their fitness values. The particle with the superior fitness value is retained for the next iteration, ensuring that only the most promising candidates are selected for progression, as detailed in (9).

$$x_i^k = \begin{cases} x_i^k & if \quad f(x_i^k) > f(x_i^{k-1}) \\ x_i^{k-1} & else \end{cases} \tag{9}$$

2.5. Stopping criterion

The update of particle positions and velocities continues iteratively until a specified stopping criterion is met. Stopping criteria are crucial for ensuring efficient algorithm performance and are generally tailored to the particular requirements of the algorithm and the problem context. In this study, the simulation is terminated once a predetermined time threshold of 40 seconds is reached.

2.6. Detection of dynamic environmental changes

As the iterative process progresses, the velocity of particles within the algorithm tends to decrease, which can lead to potential stagnation and reduced adaptability to dynamic environmental changes. To address this issue, the iPSO algorithm incorporates a reinitialization mechanism. This mechanism triggers a reinitialization of the algorithm when significant environmental changes are detected, specifically when the magnitude of the normalized power exceeds a threshold value (*Thre*), as specified in (10). The selection of this threshold is based on empirical observations across various environmental conditions and is supported by existing literature [20]. This approach ensures that the algorithm remains responsive and effective under varying conditions.

$$\left| \frac{\Delta P_{PV}}{P_{PV}^{k-1}} \right| = \left| \frac{P_{PV}^k - P_{PV}^{k-1}}{P_{PV}^{k-1}} \right| > Thre \tag{10}$$

where P_{PV}^k and P_{PV}^{k-1} are the PV output power at iterations (*k*) and (*k-1*), respectively.

3. SYSTEM OVERVIEW

Figure 3 illustrates a stand-alone photovoltaic (SAPV) system equipped with a conventional maximum power point tracking (MPPT) algorithm, typically implemented using a DC-DC boost converter. This system comprises a PV array, an MPPT algorithm module, a DC-DC converter, a pulse-width modulation (PWM) generator, and a load resistor [21]. The DC-DC converter adjusts the PV array's voltage to match the load requirements, while the MPPT algorithm regulates the converter's duty cycle (D) to manage the voltage boost. The PWM generator produces a pulse-width modulation signal based on this duty cycle, which in turn controls the on/off ratio of the switching element in the DC-DC converter to regulate the output voltage.

Figure 4 depicts the two-diode model of a PV cell, offering a detailed representation of the cell's characteristics essential for accurate simulation and analysis. This model incorporates two diodes, each accounting for different recombination losses within the cell [22]. The photo-generated current (I_{ph}), influenced by solar irradiance and temperature, flows through a circuit that includes these diodes, a series resistor (R_s), and a shunt resistor (R_{sh}), thereby affecting the cell's overall current output (I_{cell}).

$$I_{cell} = I_{ph} - I_{o1}\left[exp\left(\frac{V_{cell}+I_{cell}R_S}{a_1V_{T1}}\right) - 1\right] - I_{o2}\left[exp\left(\frac{V_{PV}+I_{cell}R_S}{a_2V_{T2}}\right) - 1\right] - \left(\frac{V_{PV}+I_{cell}R_S}{R_P}\right) \qquad (11)$$
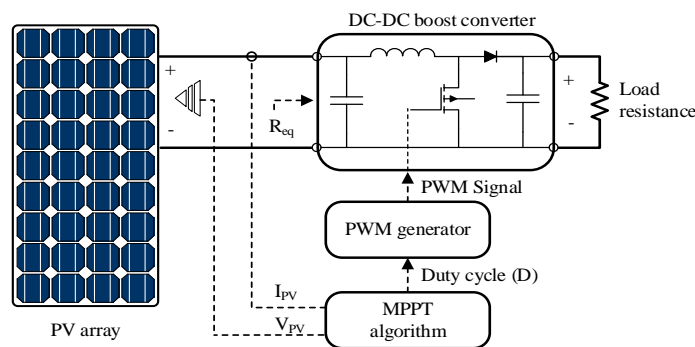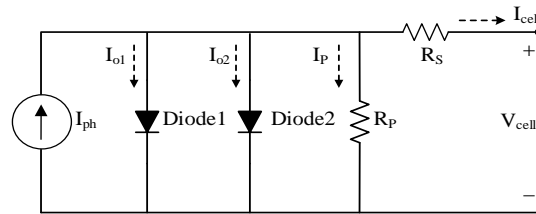

Figure 1. Block diagram of the SAPV system with MPPT

Figure 2. The two-diode PV cell model

According to (11), in this model, I_{ph} represents the photocurrent, while I_{o1} and I_{o2} denote the reverse saturation currents for diodes D_1 and D_2, respectively. V_{T1} and V_{T2} are the thermal voltages associated with diodes D_1 and D_2. The constants a_1 and a_2 are the ideality factors that influence the diodes' response to variations in temperature and current flow. V_{cell} signifies the output voltage of the solar cell. R_S refers to the series resistance, and R_P (parallel resistance) is also standardized across the cell. These parameters collectively impact the electrical characteristics and efficiency of the photovoltaic cell.

In the current research, we analyze a PV module, specifically the SPM050-P from Solar Power Mart, which consists of 36 solar cells connected in series and offers a peak power output of 50 watts (W_p). The characteristics of this module under standard test conditions (STC) are systematically presented in Table 1, including metrics such as maximum power (P_{max}), voltage at maximum power (V_{mpp}), current at maximum power (I_{mpp}), open-circuit voltage (V_{oc}), short-circuit current (I_{sc}), and the temperature coefficients for P_{max}, V_{oc}, and I_{sc}. Figure 5 illustrates the configuration of the PV array used in this study, which comprises a series arrangement of five such modules, designated as 5S1P. This setup maintains a constant temperature of 25 °C to simplify the analysis and ensure consistency in evaluating the modules' performance.

The photovoltaic (PV) array, shown in Figure 5, comprises five modules configured in two parallel strings with modules connected in series. This array is exposed to daily variations in global irradiance (G). Under uniform irradiance conditions, each module receives identical irradiance levels, resulting in a single

maximum power point (MPP) on their P-V characteristic curves. However, under partial shading conditions (PSC), different modules receive varying irradiance levels due to obstructions such as buildings, trees, or clouds. This disparity leads to multiple local maximum power points (LMPPs) alongside the global maximum power point (GMPP) on the P-V curves, complicating the MPP tracking process. To investigate this phenomenon, the research utilizes three specific irradiance patterns, as detailed in Table 2, which simulate dynamic environmental changes. The table also provides the MPP values for each pattern, offering a comprehensive evaluation of the array's performance under varying conditions.

In this study, a boost converter serves as an intermediary between the PV array and the load. This choice is based on the boost converter's significant advantages, including minimal output ripple and high efficiency. Additionally, the circuit's optimal parameters are carefully listed in Table 3 [21]. This configuration is crucial for improving overall system performance by ensuring efficient energy transfer and minimizing power loss.

Table 1. Parameters of The PV module of SPM050-P At Stc

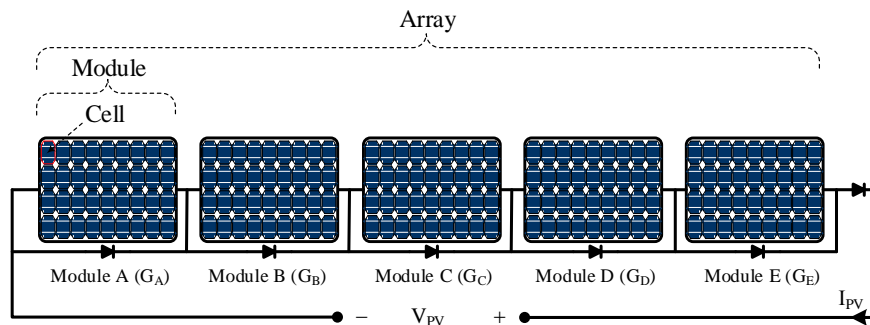| Parameters	Values
Maximum Power (P_{max})	50 W
Voltage at Pmax (V_{mpp})	18.00 V
Current at Pmax (I_{mpp})	2.78 A
Open circuit voltage (V_{oc})	21.80 V
Short circuit current (I_{sc})	2.97 A
Temperature coefficient of V_{oc}	-0.35%/°C
Temperature coefficient of I_{sc}	0.05%/°C
Temperature coefficient of power	-0.45%/°C
NOCT	47 °C
Operating temperature	25 °C

Figure 3. PV array of two parallel five modules in series

Table 2. Various irradiance patterns

Pattern	Module irradiance (G=1.0=1000 W/m²)					Maximum power point value		
	G_A	G_B	G_C	G_D	G_E		D_{MPP}	P_{MPP}
Pattern 1 (G=1000 W/m²)	1.0	1.0	1.0	1.0	1.0	MPP1	0.59	250.2 W
Pattern 2 (G=300 W/m²)	0.30	0.30	0.30	0.30	0.30	MPP2	0.24	70.7 W
Pattern 3 (PSC)	0.60	0.70	0.80	0.90	1.0	GMPP	0.45	164.6 W

Table 3. Boost converter parameters

Parameters	Values
Switching frequency, f_s	20 kHz
Load resistor, R_L	200 Ω
Boost inductor, L	2 mH
Filter capacitors, C_{in} and C_{out}	100 μF

4. SIMULATION SETUP

The investigated algorithms were simulated with the MATLAB/Simulink software platform, as shown in Figure 6. The circuit parameters are consistent with those specified in previous sections. Meanwhile, all algorithms were executed using the MATLAB function block. The photovoltaic data for all cases under investigation were generated using the PV simulator detailed in [23].
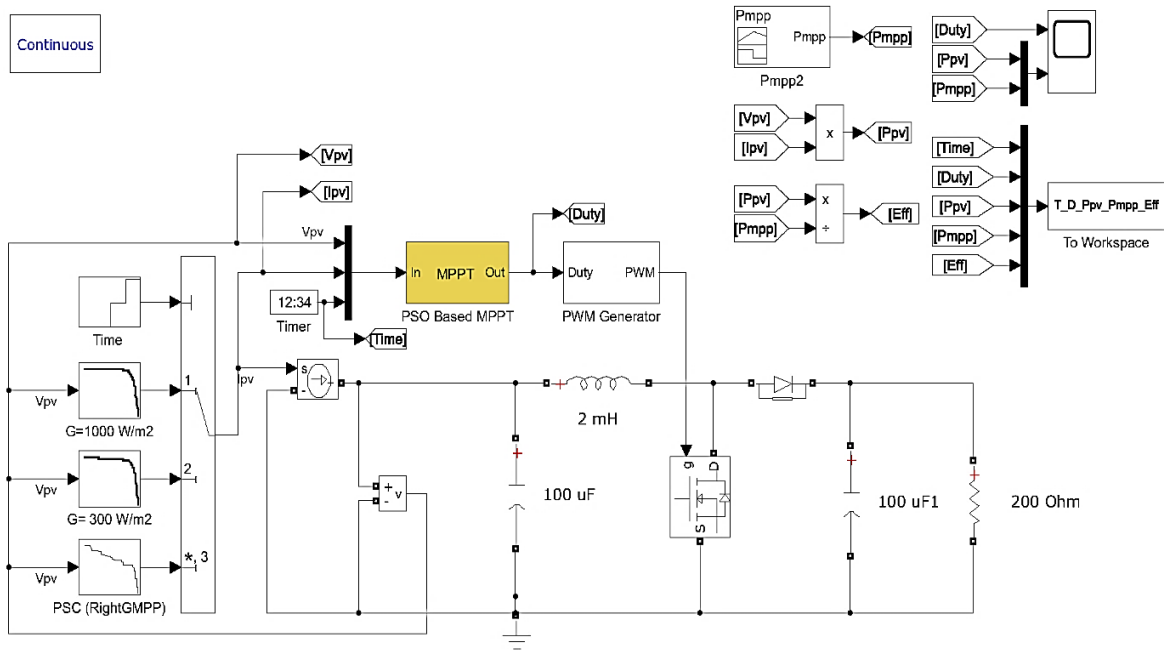
Figure 6. MATLAB/Simulink model of SAPV system with MPPT

5. HARDWARE SETUP

Figure 7 depicts an advanced hardware verification setup designed to assess MPPT algorithms in photovoltaic systems. At the heart of this arrangement is the DS1104 dSPACE controller, which manages real-time control and testing of MPPT algorithms [24], [25]. Alongside, the chroma 62000 H PV simulator is pivotal in replicating varied solar irradiance conditions, enabling rigorous evaluation of algorithm performance under controlled environmental parameters. Key measurement instruments include voltage and current sensors for accurate monitoring of electrical parameters, an oscilloscope to visualize voltage and current waveforms, and a portable DC-DC converter that ensures consistent voltage levels across system components. This comprehensive setup is essential for the precise evaluation of MPPT algorithms, ensuring theoretical advances are seamlessly translated into practical improvements in photovoltaic system efficiency.

Figure 8 shows the hardware simulation circuit created with the MATLAB/Simulink platform. The schematic integrates several system components, including analog-to-digital converters (ADCs) for voltage and current, a timer, and the PSO-based maximum power point tracking (MPPT) algorithm. These components are connected via a limited to a set of pulse-width modulation (PWM) channels, which control the output signals to keep them within predefined limits.
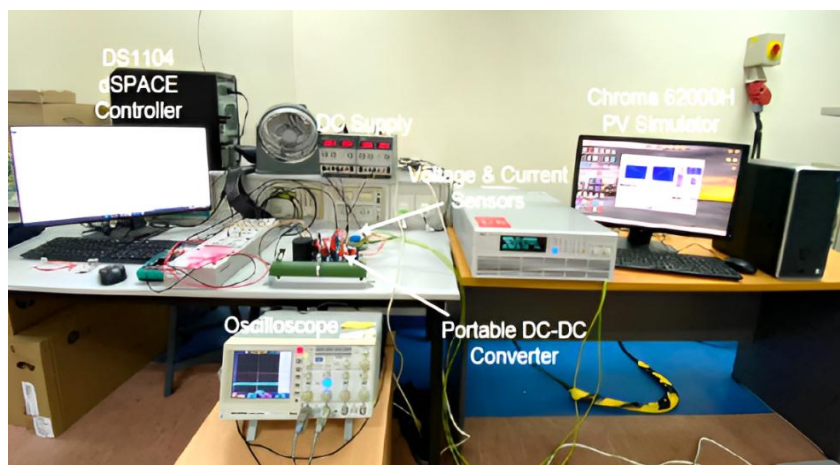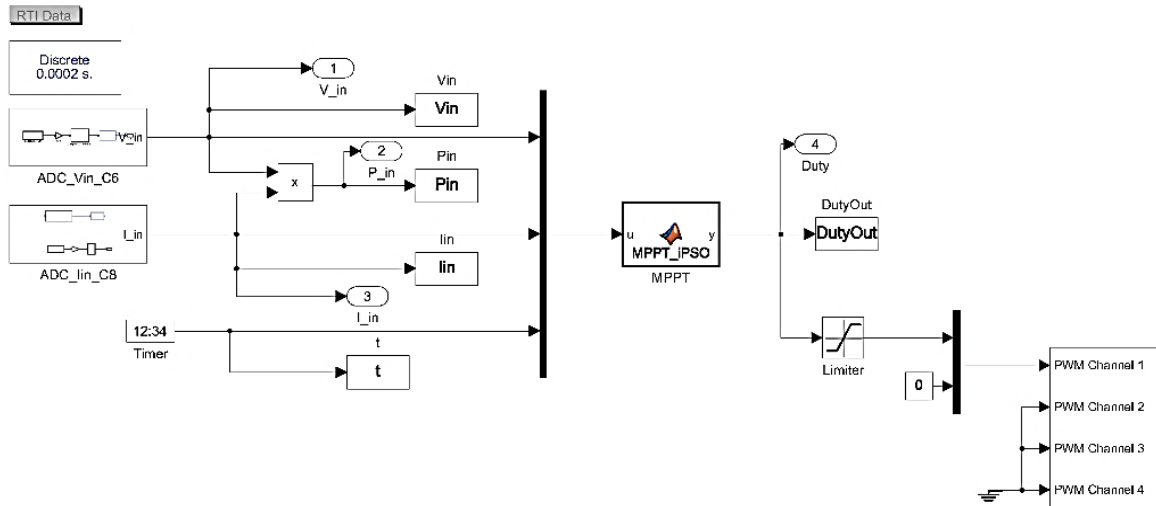

Figure 7. Hardware setup verification (MPPT)

Figure 8. Hardware Simulink circuit

Figure 9 shows the control desk main monitoring window, used to observe and analyze outputs from the hardware simulation circuit [26]. This interface offers real-time graphical representations of parameters such as voltage, current, power, and duty cycle, allowing researchers to monitor the MPPT algorithm's performance across various test conditions. This setup is essential for validating the PSO algorithm's effectiveness in optimizing the photovoltaic system's power output.
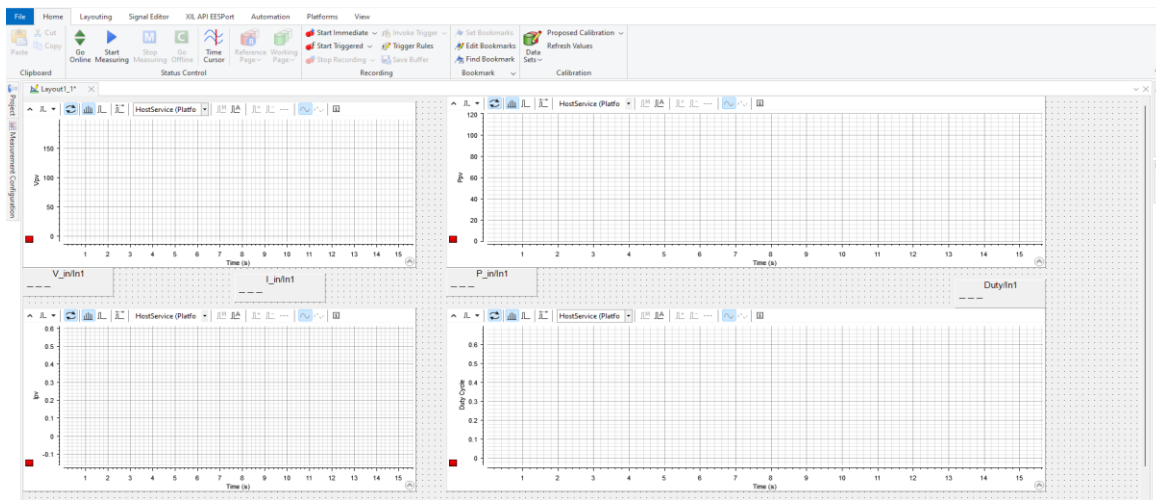

Figure 9. Control desk main monitoring window

6. RESULTS AND DISCUSSION
6.1. Simulation result

After calculating the PPV for each particle, the new position is updated as outlined in the previous section. This process will continue until convergence is achieved at MPP (D_{MPP}=0.59, P_{MPP}=250.2 W). Since $MPPT_{sampling\_time}$ is set to 0.2 s in this study, it takes 1 s ($NP{\times}MPPT_{sampling\_time}$) to finish initialization and each iteration. Figures 10 to 12 show the simulation performance of the PSO, PSO-reinit, and iPSO algorithms in tracking the maximum power point under variable environmental conditions. The data elucidates several critical aspects regarding the efficacy and adaptability of these algorithms. Firstly, the convergence metrics and efficiency figures indicate varying performance levels dependent on irradiance conditions. Under full sunlight (1000 W/m²), the iPSO algorithms achieve higher efficiencies, with MPPT efficiency reaching up to 90.69% in the best case while for conventional PSO and PSO-reinit the efficiency are 86.74% and 90.18% respectively. Conversely, under partial shading, the efficiencies tend to decrease, with the recorded efficiency

being 83.23% for PSO. This reduction emphasizes the difficulties that conventional PSO faces in adapting to fluctuating solar irradiance.

Meanwhile, the modified algorithms, PSO-reinit and iPSO, exhibit improved performance metrics compared to conventional PSO. For instance, under partial shading conditions, PSO-reinit and iPSO respond more rapidly to changes in the maximum power point, achieving efficiencies of 91.77% and 92.46%, respectively. This significant improvement over conventional PSO indicates that enhancements in the reinitialization and optimization processes of these algorithms greatly enhance their ability to manage environmental variations. Furthermore, convergence times and iteration counts reflect the responsiveness of these algorithms. Under ideal conditions with 1000 W/m² irradiance, the PSO, PSO-reinit, and iPSO algorithms converge to the optimal duty cycle in 6.4 s, 5.8 s, and 4.0 s (6.4, 5.8, and 4.0 iterations). In less optimal conditions, the iteration count increases slightly, revealing the increased complexity introduced by partial shading and the resulting strain on the algorithm's performance.
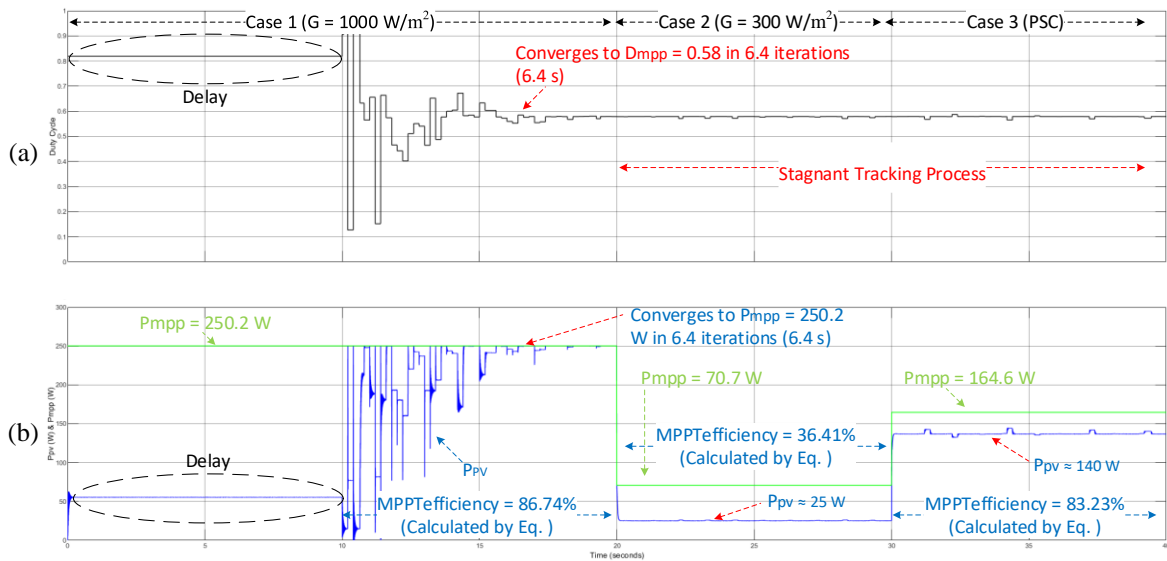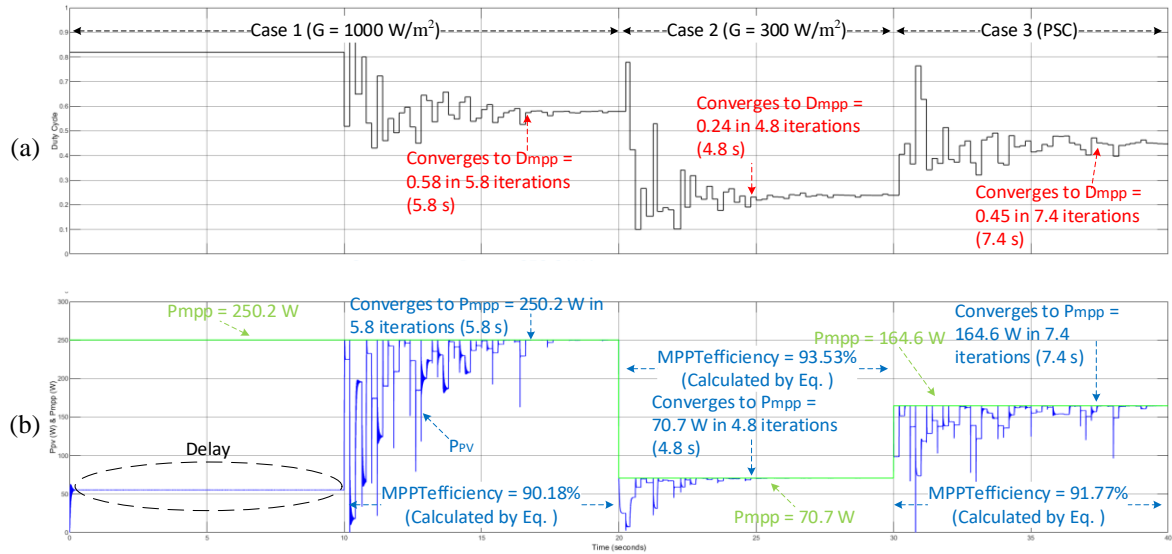

Figure 10. Simulation tracking of the conventional PSO algorithm under varying environmental conditions: (a) duty cycle and (b) PV output power

6.2. Hardware result

Full hardware tracking results for these algorithms, shown from time t=0s to t=40s in Figures 13 to 15. As indicated, the iPSO converges to the desired maximum power point (MPP) within 4.6 seconds, equivalent to 4.6 iterations, outperforming the conventional PSO and PSO-reinit variants, which required 5.6 and 5.2 iterations, respectively. The conventional PSO's limitations are evident in Cases 2 and 3, where it is unable to adapt to varying environmental conditions and remains locked at an old duty cycle (D_{mpp}= 0.59), resulting in reduced efficiencies of 35.88% and 83.15%, respectively. The MPPT speed for PSO-reinit in Case 2 is 5.2 seconds, corresponding to 5.2 iterations, whereas in Case 3, it reaches 7.4 seconds, equivalent to 7.4 iterations. Concurrently, the MPPT efficiency ($MPPT_{eff}$) for PSO-reinit in Cases 2 and 3 is approximately 92.62% and 86.36%, respectively.

The iPSO algorithm achieves significantly higher efficiencies across all scenarios due to its rapid convergence and accurate tracking. It achieves an efficiency of 90.63% under standard conditions, 94.55% under low irradiance, and 90.95% under partially shaded conditions. These improvements emphasize the value of algorithmic enhancements for ensuring reliable detection and rapid adaptation to the optimal duty cycle, reinforcing the importance of dynamic MPPT algorithms in maximizing energy yield under varying environmental conditions. Figures 10 to 15 and Table 4 provide a comparative analysis of the PSO, PSO-reinit, and iPSO algorithms, while Table 5 summarizes their average performance across the three cases studied. Simulation tracking and hardware verification offer deep insights into their applicability and efficiency in photovoltaic systems operating under variable environmental conditions.

The results consistently demonstrate the superior performance of the iPSO algorithm across several metrics, such as convergence speed and MPPT efficiency. Notably, in hardware testing for Case 2, iPSO achieved a maximum power point tracking (MPPT) efficiency of 94.55%, significantly outperforming other

algorithms. This strong performance suggests that iPSO integrates advanced adaptive mechanisms, enabling a rapid and effective response to fluctuations in irradiance and optimizing power output under diverse conditions. The consistent performance of iPSO in both simulated and practical environments highlight its robust algorithmic structure that effectively aligns theoretical predictions with actual operational outcomes. The research reveals a close correlation between simulation and hardware performance, particularly for iPSO. This alignment validates the reliability of simulation models in predicting real-world algorithm behavior.

Figure 11. Simulation tracking of the PSO-reinit algorithm under varying environmental conditions:
(a) duty cycle and (b) PV output power
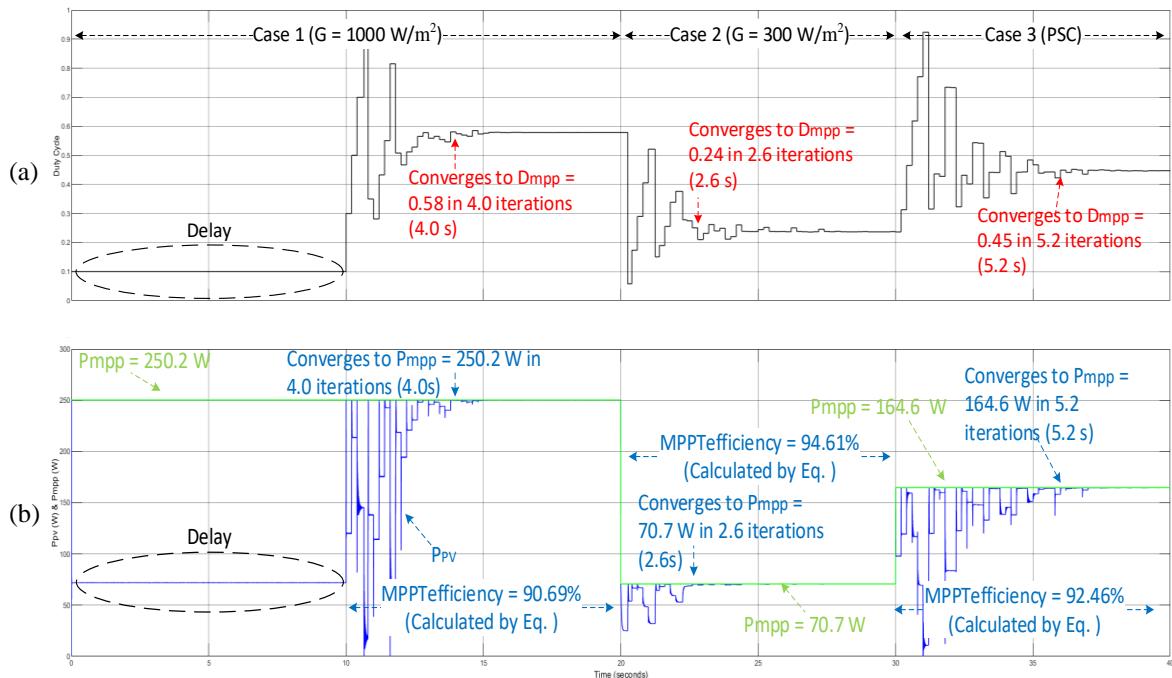
Figure 12. Simulation tracking of the iPSO algorithm under varying environmental conditions:
(a) duty cycle and (b) PV output power
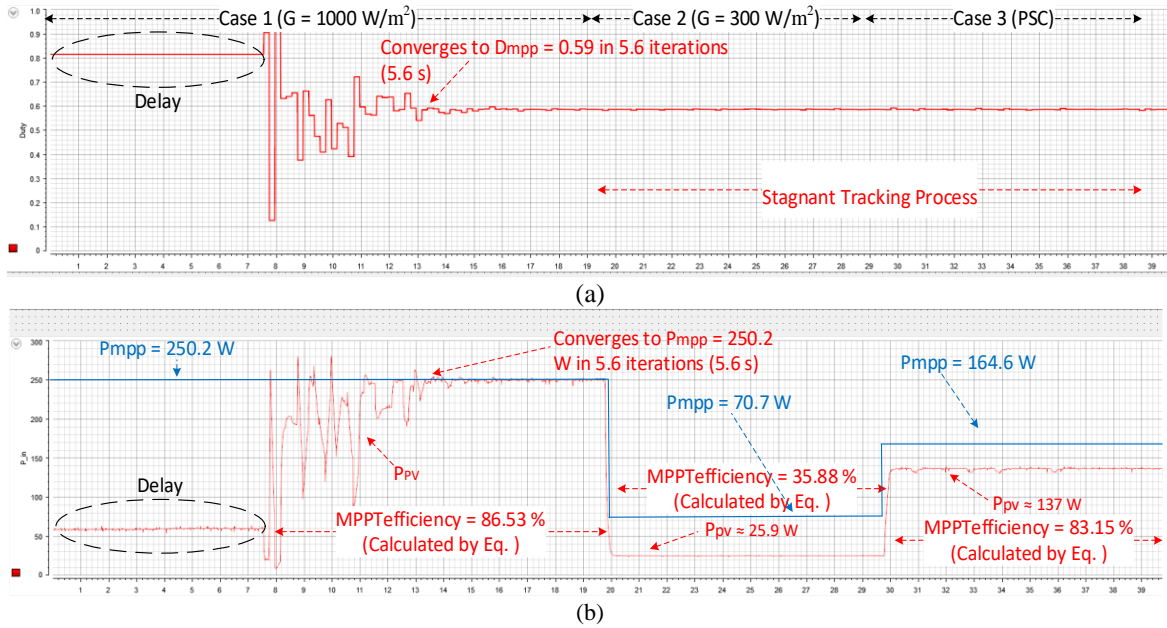
Figure 13. Hardware tracking of the conventional PSO algorithm under varying environmental conditions
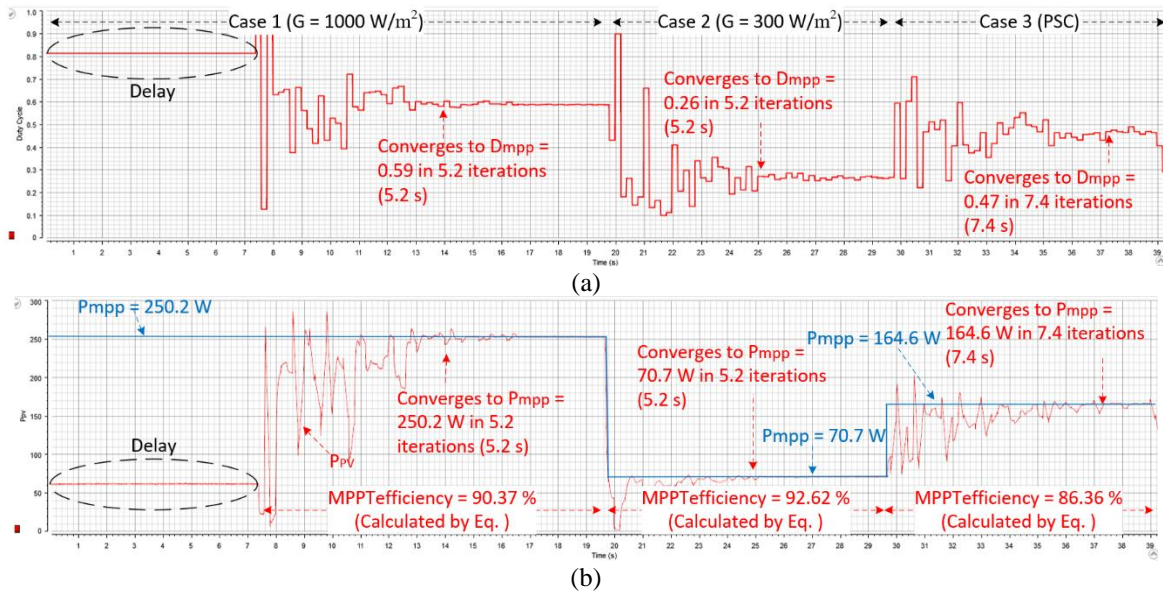(a) duty cycle and (b) PV output power

Figure 14. Hardware tracking of the PSO-reinit algorithm under varying environmental conditions
(a) duty cycle and (b) PV output power

Table 4. Overall performance results

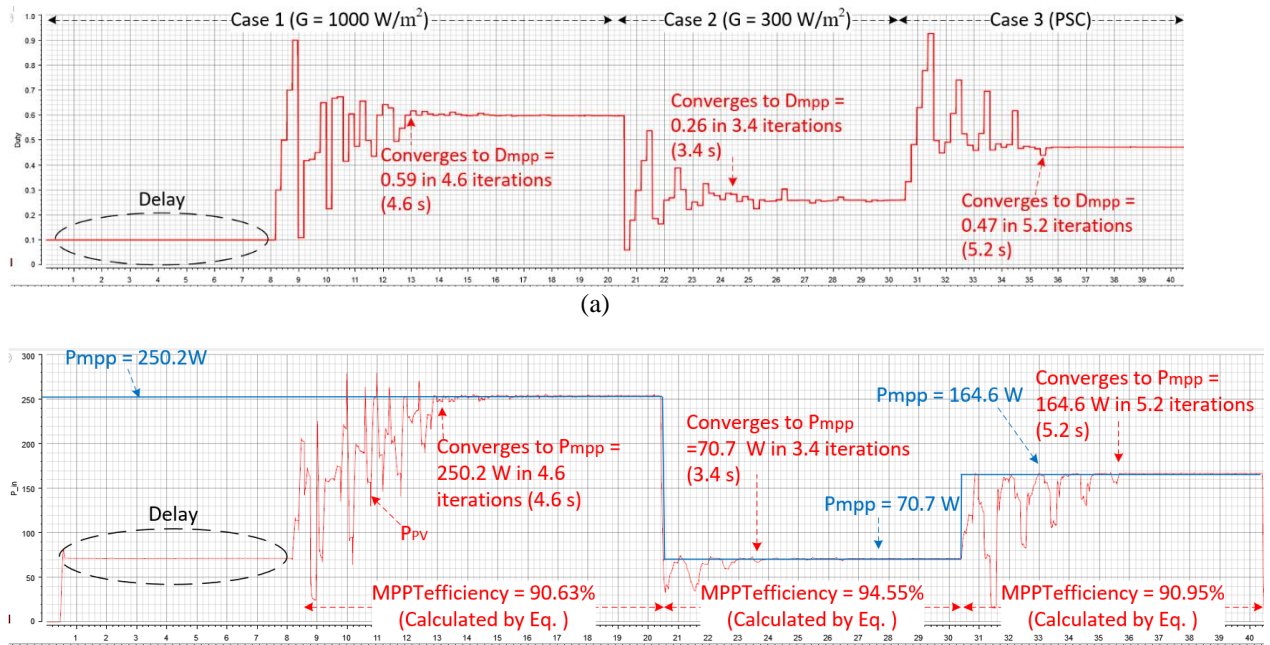| G changes	MPPT algorithm	MPPT$_{SPEED}$ (S)		MPPT$_{EFF}$ (%)	
		Simulation	Hardware	Simulation	Hardware
CASE 1 (T=10 S TO T=20 S)	PSO	6.40	5.60	86.74	86.53
	PSO-REINIT	5.80	5.20	90.18	90.37
	IPSO	4.00	4.60	90.69	90.63
CASE 2 (T=20 S TO T=30 S)	PSO	N/A	N/A	36.41	35.88
	PSO-REINIT	4.80	5.20	93.53	92.62
	IPSO	2.60	3.40	94.61	94.55
CASE 3 (T=30 S TO T=40 S)	PSO	N/A	N/A	83.23	83.15
	PSO-REINIT	7.40	7.40	91.77	86.36
	IPSO	5.20	5.20	92.46	90.95

(a)

Figure 15. Hardware tracking of the iPSO algorithm under varying environmental conditions:
(a) duty cycle and (b) PV output power

Table 5. Total average performance

MPPT algorithm	$MPPT_{SPEED}$ (S)		$MPPT_{EFF}$ (%)	
	Simulation	Hardware	Simulation	Hardware
PSO	N/A	N/A	68.79	68.52
PSO-REINIT	6.00	5.93	91.83	89.78
iPSO	3.93	4.40	92.59	92.04

7. CONCLUSION

The proposed iPSO algorithm shows superior performance in accurately tracking the GMPP in photovoltaic systems under varying environmental conditions. By dynamically adjusting inertia weight and using deterministic initialization, iPSO effectively balances exploration and exploitation, leading to faster convergence and higher efficiency than conventional PSO and PSO-reinit algorithms. Both simulation and hardware results confirm iPSO's robustness in handling partial shading conditions, rapid changes in irradiance, and uniform irradiance patterns. Achieving MPPT efficiencies exceeding 90% across various scenarios in both simulation and hardware implementations, with convergence times as short as 2.6 seconds in simulation and 3.4 seconds in hardware, iPSO stands out as a promising solution for optimizing energy extraction from PV arrays. Its capabilities ensure consistent and efficient performance across a range of operational conditions.

ACKNOWLEDGMENT

REFERENCES

[1]   L. Shang, H. Guo, and W. Zhu, "An improved MPPT control strategy based on incremental conductance algorithm," *Protection and Control of Modern Power Systems*, vol. 5, no. 1, 2020, doi: 10.1186/s41601-020-00161-z.
[2]   R. B. Bollipo, S. Mikkili, and P. K. Bonthagorla, "Critical Review on PV MPPT Techniques: Classical, Intelligent and Optimisation," *IET Renewable Power Generation*, vol. 14, no. 9, pp. 1433–1452, 2020, doi: 10.1049/iet-rpg.2019.1163.
[3]   N. Hashim and Z. Salam, "Critical evaluation of soft computing methods for maximum power point tracking algorithms of photovoltaic systems," *International Journal of Power Electronics and Drive Systems*, vol. 10, no. 1, pp. 548–561, 2019, doi: 10.11591/ijpeds.v10.i1.pp548-561.
[4]   J. P. Ram, T. S. Babu, and N. Rajasekar, "A comprehensive review on solar PV maximum power point tracking techniques," *Renewable and Sustainable Energy Reviews*, vol. 67, pp. 826–847, 2017, doi: 10.1016/j.rser.2016.09.076.
[5]   T. Esram and P. L. Chapman, "Comparison of Photovoltaic Array Maximum Power Point Tracking Techniques," *IEEE Transactions on Energy Conversion*, vol. 22, no. 2, pp. 439–449, Jun. 2007, doi: 10.1109/TEC.2006.874230.

[6]   R. Faranda, S. Leva, and V. Maugeri, "MPPT techniques for PV Systems: Energetic and cost comparison," in *2008 IEEE Power and Energy Society General Meeting - Conversion and Delivery of Electrical Energy in the 21st Century*, IEEE, Jul. 2008, pp. 1–6, doi: 10.1109/PES.2008.4596156.

[7]   D. P. Hohm and M. E. Ropp, "Comparative study of maximum power point tracking algorithms," *Progress in Photovoltaics: Research and Applications*, vol. 11, no. 1, pp. 47–62, 2003, doi: 10.1002/pip.459.

[8]   A. O. Baba, G. Liu, and X. Chen, "Classification and Evaluation Review of Maximum Power Point Tracking Methods," *Sustainable Futures*, vol. 2, 2020, doi: 10.1016/j.sftr.2020.100020.

[9]   K. Ishaque, Z. Salam, and G. Lauss, "The performance of perturb and observe and incremental conductance maximum power point tracking method under dynamic weather conditions," *Applied Energy*, vol. 119, pp. 228–236, 2014, doi: 10.1016/j.apenergy.2013.12.054.

[10]   P. Joshi and S. Arora, "Maximum power point tracking methodologies for solar PV systems – A review," *Renewable and Sustainable Energy Reviews*, vol. 70, pp. 1154–1177, 2017, doi: 10.1016/j.rser.2016.12.019.

[11]   J. Ahmed and Z. Salam, "A critical evaluation on maximum power point tracking methods for partial shading in PV systems," *Renewable and Sustainable Energy Reviews*, vol. 47, pp. 933–953, 2015, doi: 10.1016/j.rser.2015.03.080.

[12]   N. Hashim, Z. Salam, and N. F. N. Ismail, "An Improved Evolutionary Programming (IEP) Method under the EN 50530 Dynamic MPPT Efficiency Test," *CENCON 2019 - 2019 IEEE Conference on Energy Conversion*, vol. 2019-Janua, pp. 147–152, 2019, doi: 10.1109/CENCON47160.2019.8974841.

[13]   Z. Salam, Z. Ramli, J. Ahmed, and M. Amjad, "Partial shading in building integrated PV system: Causes, effects and mitigating techniques," *International Journal of Power Electronics and Drive Systems*, vol. 6, no. 4, pp. 712–722, 2015, doi: 10.11591/ijpeds.v6.i4.pp712-722.

[14]   K. Ishaque and Z. Salam, "A deterministic particle swarm optimization maximum power point tracker for photovoltaic system under partial shading condition," *IEEE Transactions on Industrial Electronics*, vol. 60, no. 8, pp. 3195–3206, 2013, doi: 10.1109/TIE.2012.2200223.

[15]   H. Deboucha, I. Shams, S. L. Belaid, and S. Mekhilef, "A fast GMPPT scheme based on Collaborative Swarm Algorithm for partially shaded photovoltaic system," *IEEE Journal of Emerging and Selected Topics in Power Electronics*, vol. 9, no. 5, pp. 5571–5580, 2021, doi: 10.1109/JESTPE.2021.3071732.

[16]   C. Worasucheep, "A Particle Swarm Optimization with Stagnation Detection and Dispersion," in *2008 IEEE Congress on Evolutionary Computation (IEEE World Congress on Computational Intelligence)*, IEEE, Jun. 2008, pp. 424–429, doi: 10.1109/CEC.2008.4630832.

[17]   N. Hashim, N. F. N. Ismail, D. Johari, I. Musirin, and A. A. Rahman, "Optimal population size of particle swarm optimization for photovoltaic systems under partial shading condition," *International Journal of Electrical and Computer Engineering*, vol. 12, no. 5, pp. 4599–4613, 2022, doi: 10.11591/ijece.v12i5.pp4599-4613.

[18]   Y. Shi and R. Eberhart, "A modified particle swarm optimizer," in *1998 IEEE International Conference on Evolutionary Computation Proceedings. IEEE World Congress on Computational Intelligence (Cat. No.98TH8360)*, IEEE, pp. 69–73, doi: 10.1109/ICEC.1998.699146.

[19]   N. Hashim, Z. Salam, N. F. N. Ismail, and D. Johari, "New deterministic initialization method for soft computing global optimization algorithms," *Indonesian Journal of Electrical Engineering and Computer Science*, vol. 18, no. 3, pp. 1607–1615, 2020, doi: 10.11591/ijeecs.v18.i3.pp1607-1615.

[20]   J. Ahmed and Z. Salam, "An Enhanced Adaptive P&O MPPT for Fast and Efficient Tracking Under Varying Environmental Conditions," *IEEE Transactions on Sustainable Energy*, vol. 9, no. 3, pp. 1487–1496, 2018, doi: 10.1109/TSTE.2018.2791968.

[21]   N. Hashim, Z. Salam, D. Johari, and N. F. N. Ismail, "DC-DC boost converter design for fast and accurate MPPT algorithms in stand-alone photovoltaic system," *International Journal of Power Electronics and Drive Systems*, vol. 9, no. 3, pp. 1038–1050, 2018, doi: 10.11591/ijpeds.v9.i3.pp1038-1050.

[22]   K. Ishaque, Z. Salam, and H. Taheri, "Simple, fast and accurate two-diode model for photovoltaic modules," *Solar Energy Materials and Solar Cells*, vol. 95, no. 2, pp. 586–594, 2011, doi: 10.1016/j.solmat.2010.09.023.

[23]   K. Ishaque, Z. Salam, and Syafaruddin, "A comprehensive MATLAB Simulink PV system simulator with partial shading capability based on two-diode model," *Solar Energy*, vol. 85, no. 9, pp. 2217–2227, 2011, doi: 10.1016/j.solener.2011.06.008.

[24]   T. Bhattacharjee, M. Jamil, and A. Azeem, "Review of dSPACE 1104 Controller and Its Application in PV," *Lecture Notes in Civil Engineering*, vol. 58, pp. 353–362, 2020, doi: 10.1007/978-981-15-2545-2_30.

[25]   A. M. Noman, K. E. Addoweesh, and H. M. Mashaly, "Simulation and dSPACE hardware implementation of the MPPT techniques using buck boost converter," *Canadian Conference on Electrical and Computer Engineering*, 2014, doi: 10.1109/CCECE.2014.6900925.

[26]   DSPACE, "dSPACE_CLP1104_Manual_201663013420." Accessed: Dec. 09, 2024. [Online]. Available: https://www.dspace.com/en/pub/home/support/documentation.cfm.

BIOGRAPHIES OF AUTHORS

Muhammad Khairul Azman Mohd Jamhari 🆔 🇬 sc ♻ obtained his B.Eng. (Hons) in Electrical Engineering from Universiti Teknologi MARA (UiTM), 2022. He is currently pursing in M.Sc. studies in Electrical Engineering at the same university. His research interests are in photovoltaic system, power electronics, and power system. He can be contacted at email: khairulazman14@gmail.com.

Norazlan Hashim received his Ph.D. degree in Electrical Engineering from Universiti Teknologi Malaysia (UTM), Skudai in 2022. He obtained his B.Eng. and M.Eng. degrees in Electrical Engineering from University of Malaya (UM), Kuala Lumpur, in 2001 and 2007, respectively. He is currently a Senior Lecturer in the School of Electrical Engineering at the Universiti Teknologi MARA (UiTM), Shah Alam, Malaysia. His research interests include maximum power point tracking techniques, power electronic converters, artificial intelligence algorithms, and PV systems. He can be contacted at email: azlan4477@uitm.edu.my.

Rahimi Baharom is a lecturer in School of Electrical Engineering, College of Engineering, Universiti Teknologi MARA, Malaysia since 2009; and he has been a senior lecturer since 2014. He received the B.Eng. degree in Electrical Engineering and the M.Eng. degree in Power Electronics, both from Universiti Teknologi MARA, Malaysia, in 2003 and 2008, respectively; and a Ph.D. degree in power electronics also from Universiti Teknologi MARA, Malaysia in 2018. He is a senior member of IEEE and also a corporate member of the Board of Engineers Malaysia and the member of the Malaysia Board of Technologists. His research interests include the field of power electronics, motor drives, industrial applications, and industrial electronics. He can be contacted at email: rahimi6579@gmail.com.

Muhammad Murtadha Othman received his B.Eng. (Hons) from Staffordshire University, England in 1998; M.Sc. from Universiti Putra Malaysia in 2000 and Ph.D. from Universiti Kebangsaan Malaysia in 2006. He is a former director for the UiTM Solar Research Institute (SRI), a centre under the project of 50MW LSSPV at Gambang, Pahang. He is also an Associate Professor at the School of Electrical Engineering, Universiti Teknologi MARA (UiTM), Malaysia. He has served as the panel assessor for research grant proposals at the Ministry of Higher Education (MOHE), Malaysia and Latvian Science Council, Europe. His area of research interests is artificial intelligence, energy efficiency, transfer capability assessment, integrated resource planning, demand side management, hybrid renewable energy, power system stability, reliability studies in a deregulated power system, power quality, and active power filters. He can be contacted at email: mamat505my@yahoo.com.